Journal of Environmental Chemical Engineering 10 (2022) 107937

Contents lists available at ScienceDirect

Journal of Environmental Chemical Engineering

journal homepage: www.elsevier.com/locate/jece

Mechanistic modeling of glycerol fermenting and sulfate-reducing processes by granular sludge under sulfidogenic conditions

X. Zhou [a], A.D. Dorado [b], J. Lafuente [a], X. Gamisans [b], D. Gabriel [a,*]

[a] GENOCOV Research Group, Department of Chemical, Biological and Environmental Engineering, Escola d'Enginyeria, Universitat Autònoma de Barcelona, 08193 Bellaterra, Spain

[b] Department of Mining, Industrial and ICT Engineering, Universitat Politècnica de Catalunya, Avinguda de les Bases de Manresa 61-73, 08242 Manresa, Spain

ARTICLE INFO

Editor: Pei Xu

Keywords:
Mechanistic model
Intermediate fermentation products
Kinetic parameters
Maximum specific uptake rates
Sulfate reducing bacteria

ABSTRACT

Glycerol can be converted to ethanol, 1,3-propanediol, formate, acetate, propionate, and inorganic carbon under anaerobic conditions through oxidative and reductive pathways in the absence and presence of sulfate. A structured mathematical model considering multiple pathways of glycerol fermentation combined with sulfate reduction was set up in this work, where three mechanisms were proposed and verified by modeling. Finally a mechanism properly predicting both glycerol fermenting and sulfate-reducing processes was chosen. Concentrations of multiple intermediates measured in batch activity tests were satisfactorily described by the model. The intermediate products of glycerol fermentation included formate, propionate, ethanol, 1,3-propanediol, and 3-hydroxypropionate (3HP). The main pathways of glycerol fermentation were the oxidative pathway to produce ethanol and the reductive pathway to produce 1,3-propanediol. The former accounted for 40.6% of the total glycerol converted whereas the latter accounted for 42.6%. 1,3-propanediol was converted to 3HP coupled to sulfate reduction. 3HP was mainly further oxidized to acetate. The kinetic parameters of maximum specific uptake rates of substrate were calibrated and then, the sulfate reduction process was validated. The confidence intervals of estimated parameters were assessed according to the Fisher information matrix (FIM) method. The low confidence intervals obtained indicated that the experimental behavior was satisfactorily described with the proposed kinetic model.

1. Introduction

Glycerol, a by-product of the biodiesel industry, is an organic waste. In order to maximize the value of crude glycerol and make it an energy source, glycerol valorization technologies can be carried out in various processes. Glycerol can be used as a valuable green solvent for catalysis and organic synthesis [1]. In addition, the direct bioconversion of glycerol to polyhydroxyalkanoates (PHAs) for bioplastics production and 1,3-propanediol for the synthesis of polyesters is also becoming a reality [2–4]. Furthermore, glycerol can be valorized biologically through fermentation processes to produce H_2 or biogas [5,6], and it has proven to be a feasible electron donor for sulfate reduction [7].

Sulfate-rich wastewaters are mainly originated from anthropogenic activities such as pulp and paper mills, food processing industries, composite tanneries, metal and coal mining [8–10]. The biotechnology of enriching and enhancing sulfate-reducing bacteria (SRB) could be a strategy for industrial and municipal sulfate-rich wastewater or SO_2-containing flue gases treatment applications [7,11]. In the anaerobic digestion process, sulfate can be reduced to sulfide by SRB with various electron donors, such as glycerol. Afterwards, sulfide can be partially oxidized to elemental sulfur in biosulfur recovery processes [7], or used for valuable metals recovery for valorization of waste effluents [11]. Overall, sulfidogenic conditions provide an alternative, more sustainable approach to the problem of flue gases emissions, changing the actual concept of production of a harmful and useless residue obtained from chemical absorption (sulfite/sulfate) into a process where potential valorization of such waste gases is carried out. Also, Paques' Sulfateq™ process (including sulfidogenic process) has been developed at full-scale for metals recovery from metal industry wastewater and acid mine drainage treatment, or even in combination with brine treatment of reverse osmosis.

Mathematical modeling has proven to be an important bioprocess engineering tool, which can be used to understand and evaluate the complexity of the sulfate reduction process in anaerobic digestion and facilitate process optimization [12,13]. Halkjaer Nielsen [14] firstly

* Corresponding author.
E-mail address: david.gabriel@uab.cat (D. Gabriel).

https://doi.org/10.1016/j.jece.2022.107937
Received 11 March 2022; Received in revised form 2 May 2022; Accepted 15 May 2022
Available online 18 May 2022

Nomenclature

$k_{m,j}$	Maximum specific substrate uptake rate of process j, mg C mg VSS^{-1} h^{-1}, or mg H_2 mg VSS^{-1} h^{-1}
$k_{s,i}$	Half saturation coefficient of component i, mg C L^{-1}, or mg S L^{-1}
R_j	Rate of process j, mg C L^{-1} h^{-1}, or mg S L^{-1} h^{-1}
S_i	Concentration of substrate component i, mg C L^{-1}, or mg S L^{-1}
$v_{i,j}$	Biochemical rate coefficient for component i in process j
X_k	Concentration of microbial trophic group k, mg VSS L^{-1}
VSS	Volatile suspended solids
FB	Fermentative bacteria
SRB	Sulfate-reducing bacteria
ASRB	Autotrophic sulfate reducing bacteria
HSRB	Heterotrophic sulfate reducing bacteria
Ace	Acetate
Eth	Ethanol
For	Formate
Gly	Glycerol
Pro	Propionate
TDS	Total dissolved sulfide
TIC	Total inorganic carbon
13PDO	1,3-propanediol
3HP	3-hydroxypropionate

discussed the sulfate kinetics in an anaerobic, sulfate-reducing biofilm reactor. A structured and comprehensive dynamic model was developed to evaluate methanogenesis and sulfate reduction in a CSTR by two groups of microorganisms, including methanogens and SRB [15]. Also, an integrated mathematical model was developed to investigate the competition between SRB and methanogens in anaerobic reactors, in which SRB were divided into acetogenic SRB, acetotrophic SRB, and hydrogenotrophic SRB [16,17]. The Anaerobic Digestion Model No.1 (ADM1) has been widely and effectively applied to describe anaerobic digestion processes in lab-scale and full-scale [18]. The extension of ADM1 to describe the sulfate reduction process has been also developed [12]. Fedorovich et al. [19] first incorporated sulfate reduction into ADM1 to predict the long-term operation of a VFAs-fed UASB reactor, which was described by multiple reaction stoichiometry, microbial growth kinetics, conventional material balances for ideally mixed reactor, liquid-gas interactions, and liquid-phase equilibrium chemistry. This model was not able to predict H_2S in the gas phase since H_2S gas-liquid mass transfer was not considered [19]. Afterwards, another extension of ADM1 with sulfate reduction for a high-strength of cane-molasses, vinasses and sulfate-rich wastewater treatment was developed to overcome the limitation of prediction of H_2S in liquid and gas phases, which included propionate and acetate as main VFAs [20]. Chen et al. [21] described a structured mathematical model based on ADM1 to describe the sulfate reduction process, which explored the long-term competitive dynamics of microorganism in 329 days of continuous operation of an ethanol-fed UASB reactor. Further efforts are needed for consolidation of existing ADM1 extensions incorporating sulfate reduction in the future.

Many studies have applied mathematical modeling to describe the bioconversion mechanism of glycerol. Mathematical models were set up to describe the pathways and kinetics of anaerobic fermentation of glycerol in batch and continuous cultures in terms of metabolic rates, enzyme-catalytic kinetics or yields, considering the consumption or production rates of glycerol, CO_2, H_2, formic acid, acetic acid, lactic acid, succinic acid, ethanol, 1,3-propanediol, and 2,3-butanediol [3,6,22,23]. Regarding sulfate reduction in anaerobic digestion, a kinetic model based on Edwards and Andrews's equation [24,25] was developed [26], who considered that glycerol was directly oxidized to acetate and inorganic carbon with sulfate reduction. However, there are many intermediate metabolites during the fermentation of glycerol, such as ethanol, 1,3-propanediol, n-butanol, 2,3-butanediol, lactate, butyrate, formate, acetate, propionate and hydrogen [27–29]. As intermediates, we refer to the compounds that can be further utilized by SRB as electron donors for sulfate reduction. Zhou et al. [30] found that glycerol was not directly oxidized to acetate but oxidized to acetate and inorganic carbon through intermediate multi-steps. In essence, glycerol was mainly reduced to 1,3-propanediol and incompletely oxidized to formate, acetate, propionate and ethanol through various metabolic pathways under sulfidogenic conditions. Although there are models describing the process of sulfate reduction with VFAs [19], ethanol [21], and glycerol [26] as carbon sources, existing models lack of a detailed description of the sulfate reduction mechanisms when other intermediates such as alcohols are produced during hydrolysis or fermentation of complex organic compounds.

The aim of this work was to develop a mechanistic model for glycerol fermentation under sulfidogenic, non-methanogenic conditions considering VFAs and alcohols as intermediate products and to estimate the kinetic parameters of anaerobic glycerol degradation and sulfate reduction processes.

2. Materials and methods

2.1. Experimental data

To investigate the mechanism of sulfate reduction using glycerol as electron donor, a mechanistic model was established using a set of data conducted in a battery of batch activity tests by Zhou et al. [30]. Activity tests performed in the absence and presence of sulfate were used considering glycerol, propionate, ethanol, 1,3-propanediol, and formate as electron donors. The initial TOC/S-SO_4^{2-} ratio of batch activity tests was set to 1.4 ± 0.1 g C/g S-SO_4^{2-}. The granular sludge for batch tests was taken from a laboratory-scale UASB reactor when the reactor was operated under non-methanogenic but sulfidogenic conditions at a sulfate inlet concentration of 250 mg S–SO_4^{2-} L^{-1} and organic carbon/-sulfate (TOC/S–SO_4^{2-}) ratio of 1.5 g C/g S–SO_4^{2-}. In the present work, activity tests performed with single organic compounds (including propionate, ethanol, 1,3-propanediol, and formate) plus sulfate were used to calibrate selected model parameters related to sulfate reduction. Activity tests performed with glycerol as the sole initial carbon source in the absence and presence of sulfate were used for glycerol fermentation parameters calibration and sulfate reduction parameters validation.

2.2. Model development

The mechanism of sulfate reduction using glycerol as the electron donor was investigated and proposed by Zhou et al. [30]. In the mechanism, glycerol was fermented to 1,3-propanediol, ethanol, formate, propionate and acetate through four pathways. SRB reduced sulfate using formate, propionate, ethanol, and 1,3-propanediol as electron donors, in which 1,3-propanediol was oxidized to acetate and propionate. However, 3-hydroxypropionate (3HP) may also be an intermediate product of glycerol degradation and 1,3-propanediol oxidation with sulfate reduction [31]. Since 3HP was not analyzed by Zhou et al. [30], this work established a mechanistic model to confirm whether 3HP played a role in glycerol degradation and 1,3-propanediol oxidation coupled to sulfate reduction. Three mechanisms were proposed herein to be simulated and verified through modeling. Mechanism I (Fig. S1A) was referred to the pathways proposed by Zhou et al. [30]. Corresponding reactions are shown in Supplementary Information from Eq.S1 to Eq.S11. As 3HP may be an intermediate product of 1,3-propanediol degradation in presence of sulfate [32,33], Mechanism II modified the possible pathway of 1,3-propanediol degradation with sulfate reduction (Fig. S1B), and the reactions were described from Eq.S13 to Eq.S15.

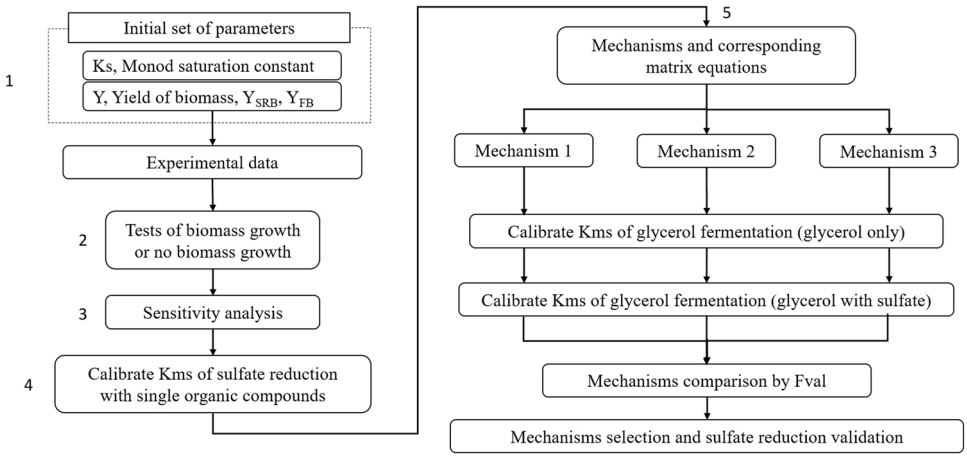

Fig. 1. Generalized procedure for parameters estimation, calibration and mechanisms selection for sulfate reduction in this work.

Since 3HP has also been reported as an intermediate product of glycerol fermentation [31], Mechanism III considered the glycerol fermentation pathway to directly produce 3HP (Fig. S1C), of which reaction is presented as Eq.S12.

Based on experimental observations discussed by Zhou et al. [30], glycerol was not used as a direct electron donor by SRB but firstly fermented to produce simpler intermediates. Then, SRB reduced sulfate through these intermediate products. In batch activity experiments [30], the sludge extracted from the UASB reactor under sulfidogenic conditions was unable to reduce sulfate using acetate and butyrate as electron donors. Although the sludge could reduce sulfate using butanol as an electron donor, butanol was not produced during glycerol degradation in this experiment. Therefore, butanol, butyrate, and acetate were not considered as electron donors for SRB in the glycerol fermentation process under sulfidogenic conditions, while ethanol, propionate, and 1, 3-propanediol were considered as electron donors for the incomplete oxidation pathway. Formate and hydrogen were also considered as electron donors for sulfate reduction process. Kinetics were based on the following assumptions:

1. The fermentation and sulfate reduction process were carried out by three types of microorganisms: X_{FB}, Fermentative bacteria; X_{HSRB}, Heterotrophic sulfate reducing bacteria; X_{ASRB}, Autotrophic sulfate reducing bacteria. Each reaction is carried out by its specific microbial group (X_{FB}, X_{ASRB}, and X_{HSRB}), as described from Eq.S1 to Eq. S15. The biomass fractions of the three types of microorganisms (77.6% of X_{FB}, 13.6% of X_{ASRB}, 8.8% of X_{HSRB}) were set up based on microbial population identification. The microbial diversity dynamics were monitored during long-term operation of the UASB reactor [34]. Results showed that SRB progressively dominated in the UASB reactor and methanogens were washed out after approximately 200 days of operation. The sludge used herein was extracted from the UASB reactor on day 538 of operation when the reactor was under sulfidogenic conditions, and the microbial diversity was analyzed [30]. Genus *Desulfobulbus* and *Desulfovibrio*, accounting for 22.4%, were SRB detected in the sludge, where the distribution of autotrophic sulfate reducing bacteria (ASRB) (13.6%) and heterotrophic sulfate reducing bacteria (HSRB) (8.8%) were estimated as recommended [17].
2. The substrate consumption rates followed a Monod-type kinetic equation. Previous studies considered a dual-substrate Monod-type kinetic for X_{ASRB} and X_{HSRB} which includes electron donors (organic carbon compounds or H_2) and the electron acceptor (sulfate) [19,21] according to Eq. (1):

$$R_j = k_{m,j} * \frac{S_i}{k_{s,i} + S_i} * \frac{S_{SO_4^{2-}}}{k_{SO_4^{2-},i} + S_{SO_4^{2-}}} * X_k \quad (1)$$

Where R_j is the kinetic rate of process j, mg C L^{-1} h^{-1}, or mg S L^{-1} h^{-1}; $k_{m,j}$ is the maximum specific uptake rate of process j, mg C mg VSS^{-1} h^{-1}, or mg H_2 mg VSS^{-1} h^{-1}; S_i is the concentration of substrate component i, mg C L^{-1}, or mg H_2 L^{-1}; $k_{s,i}$ is half saturation coefficient for the uptake of substrate component i, mg C L^{-1}, or mg H_2 L^{-1}; $k_{SO_4^{2-},i}$ is half saturation coefficient for the uptake of sulfate, mg S L^{-1}; $S_{SO_4^{2-}}$ is the concentration of sulfate, mg S L^{-1}; X_k is the concentration of microbial trophic group k, mg VSS L^{-1}.

The half saturation coefficient of sulfate for X_{ASRB} and X_{HSRB} was 3.2 mg S L^{-1} and 6.7 mg S L^{-1}, respectively, according to Fedorovich et al. [19]. In this work, the sulfate concentration in all experiments of Zhou et al. [30] were higher than 30 mg S L^{-1} at the end of the experiment, far higher than the half saturation coefficient for sulfate. Under carbon limiting conditions, kinetic equations were considered only dependent on organic electron donors for X_{FB}, X_{ASRB}, X_{HSRB} according to Eq. (2):

$$p_j = k_{m,j}' * \frac{S_i}{k_{s,i} + S_i} * X_k \quad (2)$$

3. The effect of pH on biomass growth rates was not included, since K_2HPO_4 was used in all the experiments as pH buffer in all batch test. The pH ranged between 7.2 and 8.4 during the cultivation. Sulfidogenic activity can be carried out in a wide pH range (5.0–10.0), and the optimal pH has been reported in the range of pH 7.0–8.5 [35,36].
4. The inhibition effect of H_2S as product of sulfate reduction was considered in previous models [20], which estimated that 50% inhibitory concentration of free H_2S for SRB was 240 mg S-H_2S L^{-1}. Kalyuzhnyi and Fedorovich [17] reported that the concentration of free H_2S that produced a 50% inhibition on growth rates for FB, ASRB, and HSRB were 518, 268, 517 mg S-H_2S L^{-1}, respectively. Free H_2S detected in the experiments in Zhou et al. [30] ranged from 0 to 76 mg S-H_2S L^{-1}. Thus, free H_2S inhibition in this work was not considered. The maximum tolerance concentrations for *Clostridium butyricum* and *Klebsiella pneumoniae* are 0.35 g L^{-1} for undissociated acetic acid, 10.1 g L^{-1} for total butyric acid, 16.6 g L^{-1} for ethanol, 71.4 g L^{-1} for 1,3-propanediol, and 187.6 g L^{-1} for glycerol, respectively [37]. These values are far beyond the concentration used in this work, so the inhibitory effect of substrate was also not considered.

According to biochemical processes mentioned before and the 14

Table 1
Initial inputs of stoichiometric and kinetic parameters used in the model.

Parameter	Name	Value	Unit	Reference
Y_{FB}	Yield of FB	0.132	g VSS g C^{-1}	[20]
Y_{HSRB}	Yield of HSRB	0.077	g VSS g C^{-1}	[20]
Y_{ASRB}	Yield of ASRB	0.288	g VSS g H_2^{-1}	[20]
Fermentation process				
$k_{s,for,FB}$	Half saturation coefficient for the uptake of formate by FB	0.03	mg C L^{-1}	[39]
$k_{s,gly}$	Half saturation coefficient for the uptake of glycerol by FB	1.96	mg C L^{-1}	[37]
Sulfate reduction process				
$k_{s,pro}$	Half saturation coefficient for the uptake of propionate by HSRB	79	mg C L^{-1}	[17]
$k_{s,for,HSRB}$	Half saturation coefficient for the uptake of formate by HSRB	53	mg C L^{-1}	[17]
$k_{s,eth}$	Half saturation coefficient for the uptake of ethanol by HSRB	45	mg C L^{-1}	[38]
$k_{s,13PDO}$	Half saturation coefficient for the uptake of 1,3-propanediol by HSRB	45	mg C L^{-1}	This work
$k_{s,H2}$	Half saturation coefficient for the uptake of H_2 by ASRB	0.00625	mg H_2 L^{-1}	[17]

components monitored in the experiments, the biochemical rate coefficients ($v_{i,j}$) and kinetic rate equations (R_j) are listed in Supplementary Information (Table S1) in a complete format.

2.3. Modeling procedure

The procedure carried out for the estimation of model parameters and determination of the mechanisms linked to glycerol fermentation coupled to sulfate reduction is illustrated in Fig. 1. The procedure involves five steps as follows.

In Step 1, kinetic parameters were set up, including half saturation coefficients (ks), and biomass yields (Y) as listed in Table 1. Among them, the half saturation coefficient for 1,3-propanediol ($k_{s,13PDO}$) by HSRB was not found in previous studies. In this work, the initial value of $k_{s,13PDO}$ was selected as 45 mg C L^{-1} based on that reported for ethanol [38] as both ethanol and 1,3-propanediol belong to primary alcohols and can be degraded by HSRB [17].

As tests performed by Zhou et al. [30] lasted around 100–120 h, in Step 2 the model was tested to verify if biomass growth was significant in the batch activity tests and, thus, a variable biomass concentration should be included in the model. Two-tailed Student's t-test was also used to statistically evaluate the significant difference between experimental data and results obtained from model fitting. P value < 0.05 was considered to be statistically significant.

In Step 3, a sensitivity analysis was performed to identify the most sensitive kinetic parameters in these biochemical processes. Sensitivity analysis can prioritize and analyze the impact of model parameters on process variables, thereby providing effective information for model calculation. Sensitivity functions were described by Dochain and Vanrolleghem [40] to determine the significance of kinetic parameters, which used the finite difference approximation. Sensitivity functions have been applied in previous studies, which is based on the change of measurable process variables under the disturbance of model parameters caused by a perturbation value δ [20,21]. The perturbation δ of each parameter was chosen and the sensitivity of the output caused by the perturbation of parameters was calculated according to Eq. (3):

$$\Gamma_{i,j} = \frac{\partial y_j / y_j}{\partial \theta_i / \theta_i} = \frac{(y_j(\theta_i + \delta \cdot \theta_i) - y_j(\theta_i)) / y_j(\theta_i)}{(\delta \cdot \theta_i)/\theta_i} \quad (3)$$

Where $\Gamma_{i,j}$ is the dimensionless sensitivity value of output y_j with respect to the kinetic parameters θ_i (such as $k_{m,j}$, ks); $\theta_i + \delta \bullet \theta_i$ is the perturbation parameter value. The sensitivity values for each parameter were calculated as $\sum\Gamma_{i,j}$ (show as % in respect to the total $\sum\sum\Gamma_{i,j}$) and arranged in descending order.

In Step 4, the maximum specific uptake rates ($k_{m,j}$) for sulfate reduction were calibrated from activity tests with single organic compounds, including formate, propionate, ethanol and 1,3-propanediol. The stoichiometry corresponding to propionate and ethanol are shown in Eq.S8 ($k_{m,pro}$) and Eq.S9 ($k_{m,eth}$), respectively. The stoichiometry corresponding to formate include Eq.S5 ($k_{m,for,FB}$), Eq.S6 (k_{m,H_2}) and Eq. S7 ($k_{m,for,HSRB}$). When 1,3-propanediol was used as an electron donor, the sulfate reduction stoichiometry corresponds to Eq.S10 ($k_{m,13PDO1}$) and Eq.S11 ($k_{m,13PDO2}$) in Mechanism I, and corresponds to Eq.S13 ($k_{m,13PDO3}$), Eq.S14 ($k_{m,3hp1}$), and Eq.S15 ($k_{m,3hp2}$) in Mechanisms II and III.

In Step 5, the maximum specific uptake rates ($k_{m,j}$) for glycerol fermentation were calibrated from activity tests with glycerol as the carbon source. Equations Eq.S1 ($k_{m,gly1}$), Eq.S2 ($k_{m,gly2}$), Eq.S3 ($k_{m,gly3}$), Eq.S4 ($k_{m,gly4}$) provide the stoichiometry related to the fermentation pathway of glycerol in Mechanism I and II. Mechanism III included the fermentation of glycerol to produce 3HP, corresponding to Eq.S12 ($k_{m,gly5}$). In this case, calibration was performed for each one of the three proposed mechanisms. This step also determined the optimal mechanism of the glycerol degradation pathway (I, II or III) as well as validated the kinetic rates of sulfate reduction processes by comparing the objective function value (Fval) of each one of the three mechanisms.

Fval is the minimum value of the objective function in each simulation. The smaller the value, the smaller the difference between experimental data and model predictions. Fminsearch function, a MATLAB algorithm based on a multidimensional unconstrained nonlinear minimization (Nelder-Mead), was used to minimize the error between model and experimental data and find out Fval that lead to optimum model parameters, as given in Eq. (4).

$$\text{Fval} = \sum_{i=1}^{N} |C_E - C_M| \quad (4)$$

C_E is the experimental concentration in all sulfate reduction experiments performed with glycerol, formate, propionate, ethanol, and 1,3-propanediol as the carbon source, and all fermentation experiments performed with glycerol as the carbon source; C_M is the concentration predicted by the model; and N is the total number of data sets, including organic carbon compounds and sulfate in all the experiments for model fitting. The set of the differential equations was solved by ode45 function (based on Runge-Kutta method with a variable time step) in MATLAB. All simulations and calibrations were implemented in MATLAB 2015a. Subsequently, the optimal mechanism obtained through the above steps was analyzed by two-tailed Student's t-test between the experimental data and the modeling results.

In order to evaluate the calibrated parameters and the quality of the estimation, the confidence intervals of estimated kinetic parameters were calculated based on the Fisher Information Matrix (FIM) method [40,41]. The FIM method has been widely applied to evaluate the reliability of estimated parameters in modeling of biofiltration on gas treatment [42], aerobic biological sulfide oxidation [43], and sulfate-rich wastewater treatment [20]. The FIM method is based on the calculation of the inverse of the covariance matrix, which takes into account the output sensitivity functions and the measurement errors, the quantity and quality of experimental data. The higher the FIM value the lower the standard errors estimated.

3. Results and discussion

3.1. Parameters estimation and sensitivity analysis

Microbial biomass growth was estimated in 120 h batch tests performed with glycerol as electron donor in absence of sulfate. The

Table 2
Model sensitive parameters arranged in descending order from the first to the last in Mechanism I, II, and III (perturbation factor was set as ± 10%).

	Parameters						
Mechanism I	$k_{m,gly4}$	$k_{s,eth}$	$k_{m,gly3}$	$k_{m,eth}$	$k_{m,for,FB}$	$k_{m,H2}$	$k_{m,13PDO1}$
(δ = 10%)	$k_{m,gly1}$	$k_{m,13PDO2}$	$k_{m,pro}$	$k_{s,pro}$	$k_{m,gly2}$	$k_{s,13PDO}$	$k_{m,for,HSRB}$
	$k_{s,for,HSRB}$	$k_{s,H2}$	$k_{s,gly}$	$k_{s,for,FB}$			
Mechanism I	$k_{m,eth}$	$k_{m,gly3}$	$k_{m,gly4}$	$k_{m,for,FB}$	$k_{m,H2}$	$k_{m,13PDO1}$	$k_{s,eth}$
(δ = −10%)	$k_{m,gly1}$	$k_{m,13PDO2}$	$k_{m,pro}$	$k_{s,pro}$	$k_{m,gly2}$	$k_{s,13PDO}$	$k_{m,for,HSRB}$
	$k_{s,for,HSRB}$	$k_{s,H2}$	$k_{s,gly}$	$k_{s,for,FB}$			
Mechanism II	$k_{m,gly3}$	$k_{m,gly4}$	$k_{s,eth}$	$k_{m,13PDO3}$	$k_{m,eth}$	$k_{m,for,FB}$	$k_{m,H2}$
(δ = 10%)	$k_{s,3HP,FB1}$	$k_{m,gly1}$	$k_{m,3HP1}$	$k_{s,pro}$	$k_{m,for,HSRB}$	$k_{m,3HP2}$	$k_{m,pro}$
	$k_{s,for,HSRB}$	$k_{m,gly2}$	$k_{s,13PDO}$	$k_{s,3HP,FB2}$	$k_{s,for,FB}$	$k_{s,gly}$	$k_{s,H2}$
Mechanism II	$k_{m,eth}$	$k_{m,13PDO3}$	$k_{m,gly3}$	$k_{m,gly4}$	$k_{m,for,FB}$	$k_{m,H2}$	$k_{s,eth}$
(δ = −10%)	$k_{m,gly1}$	$k_{m,3HP1}$	$k_{s,3HP,FB1}$	$k_{m,pro}$	$k_{m,for,HSRB}$	$k_{s,pro}$	$k_{m,3HP2}$
	$k_{s,for,HSRB}$	$k_{m,gly2}$	$k_{s,13PDO}$	$k_{s,3HP,FB2}$	$k_{s,for,FB}$	$k_{s,gly}$	$k_{s,H2}$
Mechanism III	$k_{s,eth}$	$k_{m,gly3}$	$k_{m,gly4}$	$k_{m,13PDO3}$	$k_{m,eth}$	$k_{m,gly5}$	$k_{s,3HP,FB1}$
(δ = 10%)	$k_{m,for,FB}$	$k_{m,H2}$	$k_{m,gly1}$	$k_{s,for,HSRB}$	$k_{s,for,FB}$	$k_{m,for,HSRB}$	$k_{m,3HP1}$
	$k_{s,pro}$	$k_{m,pro}$	$k_{m,3HP2}$	$k_{m,gly2}$	$k_{s,H2}$	$k_{s,gly}$	$k_{s,13PDO}$
	$k_{s,3HP,FB2}$						
Mechanism III	$k_{m,H2}$	$k_{m,for,FB}$	$k_{m,gly3}$	$k_{m,eth}$	$k_{m,13PDO3}$	$k_{m,gly5}$	$k_{s,for,FB}$
(δ = −10%)	$k_{m,gly4}$	$k_{s,3HP,FB1}$	$k_{s,eth}$	$k_{m,3HP2}$	$k_{s,H2}$	$k_{s,for,HSRB}$	$k_{s,gly}$
	$k_{m,gly2}$	$k_{s,13PDO}$	$k_{s,pro}$	$k_{m,for,HSRB}$	$k_{m,pro}$	$k_{m,3HP1}$	$k_{m,gly1}$
	$k_{s,3HP,FB2}$						

experimental data and the modeled profiles both considering the influence of biomass growth or no-biomass growth for the three proposed mechanisms is shown in Supplementary Information (Fig. S2). In mechanism I (Fig. S2A and S2B), through Student's t-test, there was no significant difference between the experimental data and the model prediction whether the biomass growth was considered or not. Same results were observed in mechanism II (Fig. S2C and S2D). In mechanism III, there was a significant difference between the experimental data and model predictions for ethanol (Fig. S2E) when biomass growth was considered. However, there was not a significant difference when biomass yield was not considered (Fig. S2F). Therefore, combining the experimental data and model predictions in the three mechanisms, the batch tests did not consider biomass growth in this work for none of three mechanisms considered.

In order to identify the most sensitive kinetic parameters, a sensitivity analysis was performed for the three mechanisms proposed and the experimental data from activity tests with glycerol as electron donor and sulfate as electron acceptor. Output variables selected to assess the sensitivity were the concentrations of sulfate, total dissolved sulfide (TDS), propionate, acetate, formate, H_2, total inorganic carbon (TIC), 1,3-propanediol, ethanol, 3HP and glycerol along the batch activity test. The parameters of the sensitivity analysis included all half saturation coefficients and maximum specific uptake rates involved in the three proposed mechanisms. The perturbation factor (δ), which is defined as the percentage change of a model parameter with respect to a reference value of that parameter, was set to ± 10%.

Simulations carried out allowed ranking the model parameters in descending order of sensitivity, as shown in Table 2. The maximum specific uptake rates had a higher impact on process variables than half saturation coefficients in general.

The sensitivity values ($\sum\Gamma_{i,j} / \sum\sum\Gamma_{i,j}$, %) for the four most sensitive parameters in each mechanism are shown in Fig. 2, when the perturbation factor δ was set to 10%. Fig. 2 shows that $k_{m,gly4}$, $k_{m,gly3}$, $k_{m,eth}$, and $k_{s,eth}$ were the most sensitive parameters for mechanism I, which are related to reactions in Eq.S3, Eq.S4, and Eq.S9. In Mechanism I, II and III, $k_{m,gly3}$, $k_{m,gly4}$, $k_{s,eth}$, and $k_{m,13PDO3}$ were the most sensitive parameters, which are related to reactions Eq.S3, Eq.S4, Eq.S9 and Eq.S13. Fig. 2 also shows the sensitive model parameters for each process variable. The process variable S_{eth} was highly sensitive to parameters $k_{m,eth}$ and $k_{s,eth}$. Parameters $k_{m,gly3}$ and $k_{m,gly4}$ simultaneously affected the process variable S_{eth} and S_{13PDO}, while $k_{m,13PDO3}$ mainly affected the process variable S_{3HP} and S_{13PDO} at the same time. When the perturbation factor δ was set to − 10%, the sensitivity values of the four most sensitive parameters in each mechanism were similar to the results when the perturbation factor δ was set to 10%, as shown in Fig. S3. The most sensitive parameters were the maximum specific uptake rates in the three mechanisms, including $k_{m,gly3}$, $k_{m,gly4}$, $k_{m,eth}$, $k_{m,for,FB}$, $k_{m,13PDO3}$ and $k_{m,H2}$. Therefore, all the substrates of the maximum specific uptake rates were calibrated and half saturation coefficients mainly referred to previous studies.

Based on the sensitivity analysis results, the half saturation coefficient for the uptake of ethanol ($k_{s,eth}$) was one of the most sensitive parameters in the sulfate reduction process with glycerol as electron donor. In this work, $k_{s,eth}$ was initially taken from literature since no specific tests were carried out for its determination. Gonzalez-Silva et al. [38] reported a $k_{s,eth}$ = 45 mg C L^{-1}. However, the lowest experimental ethanol concentration detected in Zhou et al. [30] was 4.3 mg C L^{-1}, and the ethanol consumption rate was not limited. Thus, simulations with a $k_{s,eth}$ = 45 mg C L^{-1} (Fig. S4A) and $k_{s,eth}$ = 5 mg C L^{-1} (Fig. S4B) were compared. Fig. S4A shows a significant difference ($P < 0.05$) between model prediction and experimental data for ethanol consumption after 24 h, whereas no significant difference in ethanol between model prediction and experimental data was found in Fig. S4B. Then, $k_{s,eth}$ was adjusted to 5 mg C L^{-1} in this work. Similarly, $k_{s,13PDO}$ was initially set to 45 mg C L^{-1}, but the consumption of 1,3-propanediol in the model was slower than the experimental data (Fig. S4A). Thus, $k_{s,13PDO}$ was also set to 5 mg C L^{-1} to provide a better description of 1,3-propanediol consumption (Fig. S4B). The half saturation coefficients for all other compounds were set as those provided in literature (Table 1). In any case, further research on the half saturation coefficient of each compound is warranted.

3.2. Model calibration of sulfate reduction mechanisms with single organic compounds

As described by Zhou et al. [30], no methane was produced during the batch tests in which sulfate reduction was studied. Consequently, the model did not consider methanogenesis. Additionally, batch experiments showed that when acetate was fed as carbon source, there was neither methane production nor sulfate reduction. Consequently, acetotrophic SRB were not included as model variable.

The mathematical model established in this work was first calibrated for the maximum specific uptake rates of batch activity tests with single organic compounds, including propionate, formate, ethanol and 1,3-propanediol. The pathways for sulfate reduction using propionate, ethanol and formate as electron donors are described in Eq.S8, Eq.S9, and Eq.S7, respectively. The sulfate reduction process was the same among the three proposed mechanisms using these three electron

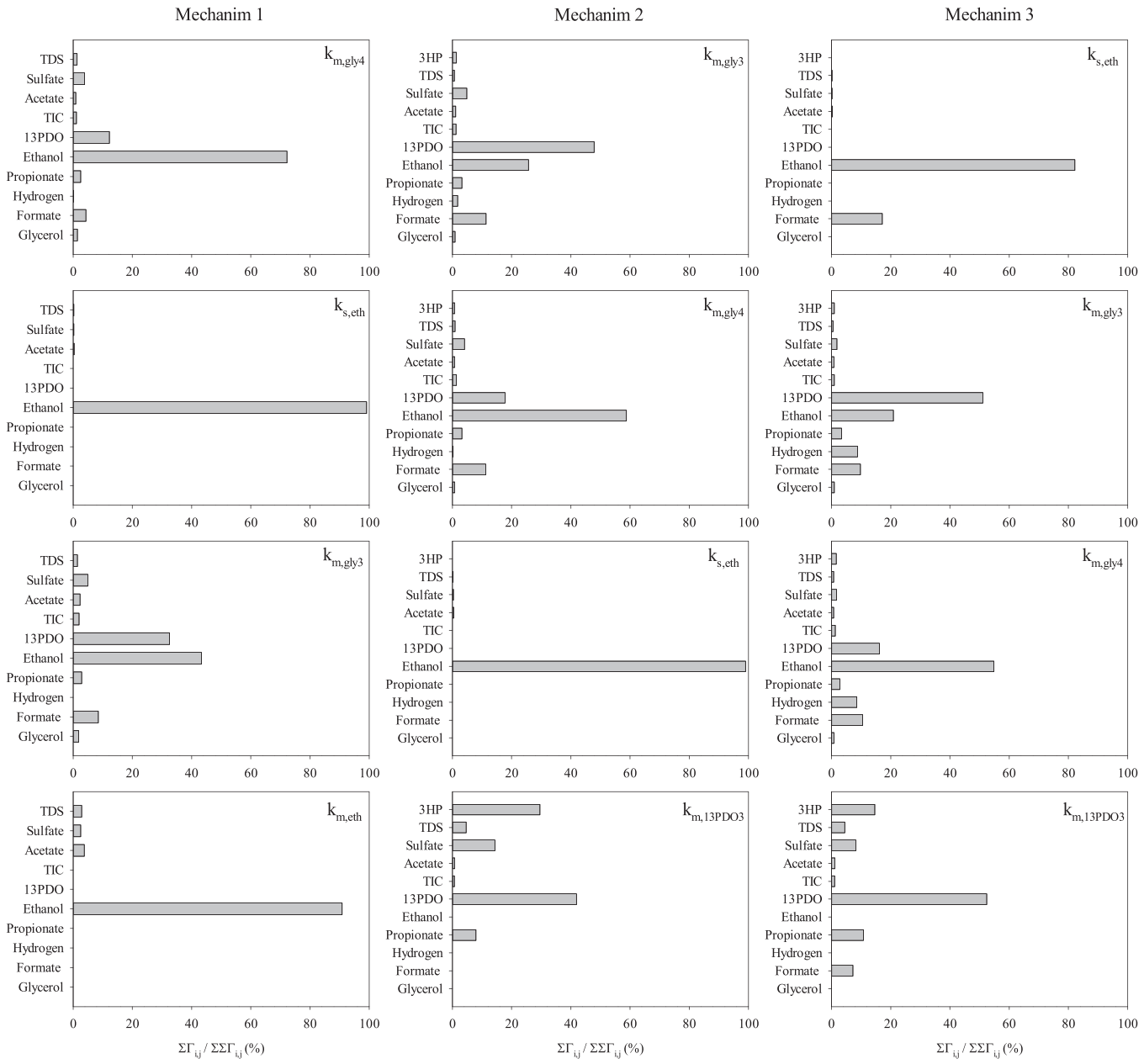

Fig. 2. Most sensitive model parameters arranged in descending order from top to bottom for each one of the three mechanisms (the perturbation factor δ was set as 10%). Each Y axis shows the output variables selected.

donors.

Predicted concentrations by the model of the abovementioned batch activity tests with the calibrated $k_{m,j}$ are shown in Fig. 3. According to Student's t-test, no significant differences were found between experimental data and model predictions for these activity tests. The maximum specific uptake rates for single organic compounds ($k_{m,j}$) involved in the sulfate reduction process using propionate, formate, ethanol and 1,3-propanediol as electron donors were estimated (Table 3). As can be observed in Table 3, there was a difference between the $k_{m,j}$ of sulfate reduction calibrated in this work and the $k_{m,j}$ in previous studies. Activity tests were conducted under the coexistence of methanogenesis and sulfidonegenesis in previous studies, which allowed SRB and methanogens to coexist in reactors. When these carbon compounds were used as electron donors, they were used not only for sulfate reduction, but also for biogas production. The batch activity tests herein were performed under sulfidogenic conditions instead of methanogenic conditions. These electron donors were not consumed through biogas production in our work, but were only used for sulfate reduction. The microbial adaptability of sludge culture resulted in SRB enrichment in the reactor, which may contribute to the difference between this experiment and previous studies.

When 1,3-propanediol is used as carbon source to reduce sulfate and the production of 3HP is not considered, the degradation process of 1,3-propanediol can be described from Eq.S10 and Eq.S11 (Mechanism I). Its model fitting results are shown in Fig. 4. It is worth mentioning that 3HP may be used as an intermediate product in the degradation process of glycerol and 1,3-propanediol [31,33]. When 3HP is considered as an intermediate product of 1,3-propanediol degradation, the process is followed by Eq.S13, Eq.S14, and Eq.S15 (Mechanisms II and III). The degradation of 1,3-propanediol with sulfate reduction process were same in Mechanism II and III, and the model fitting results are shown in Supplementary Information (Fig. S5). Through the Student's t-test, there was no significant difference between model and experimental data in these three mechanisms. Their corresponding maximum specific uptake

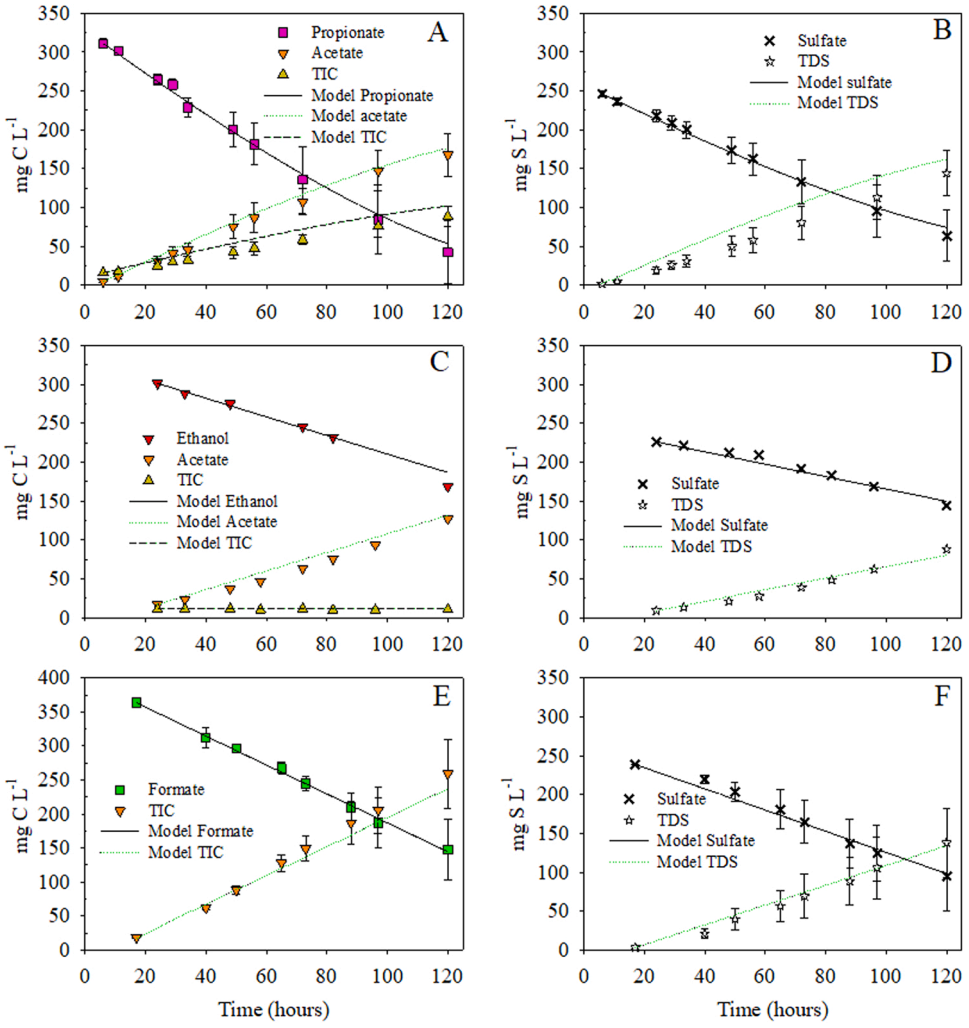

Fig. 3. Experimental and model simulation of sulfate reduction using propionate (A and B), ethanol (C and D), and formate (E and F) as electron donors. A, C, and E show the degradation process of organic carbon compounds; B, D, and F show sulfate reduction process. Data points illustrate the experimental data. Smooth lines represent model predictions.

Table 3
Maximum specific uptake rates of propionate, ethanol and formate calibrated in this work and found in literature.

Parameters	In this work	Literature
$k_{m,pro,HSRB}$ (mg C mg VSS^{-1} h^{-1})	9.96 (± 0.08)	0.44[a], 0.24[b]
$k_{m,eth,HSRB}$ (mg C mg VSS^{-1} h^{-1})	4.49 (± 0.11)	0.003[c]
$k_{m,H2,ASRB}$ (mg H_2 mg VSS^{-1} h^{-1})	0.47 (± 0.03)	0.46[a], 0.20[b]
$k_{m,for,FB}$ (mg C mg VSS^{-1} h^{-1})	3.02 (± 0.01)	0.56[d]
$k_{m,for,HSRB}$ (mg C mg VSS^{-1} h^{-1})	3.78 (± 0.12)	0.16[e]

Note: Confidence interval estimated through FIM is presented in parentheses.
[a] Barrera et al. [20].
[b] Fedorovich et al. [19].
[c] Gonzalez-Silva et al. [38].
[d] Vignolle et al. [44].
[e] Bijmans et al. [45].

rates obtained according to different degradation pathways are shown in Table 4. To the best of our knowledge, this is the first work that used 1, 3-propanediol as an electron donor to calibrate its maximum specific uptake rate for sulfate reduction.

3.3. Model calibration with glycerol as carbon source

3.3.1. Model calibration for glycerol fermentation

In the absence of sulfate, each $k_{m,j}$ of glycerol fermentation routes based on Mechanism I were calibrated through Eq.S1 to Eq.S4, as shown in Fig. S2B. Through the Student's t-test, it is found that there was no significant difference between the model and experimental data of the glycerol degradation process. The maximum specific uptake rates of glycerol fermentation ($k_{m,gly}$) in absence of sulfate are shown in Table S2. Estimated by the $k_{m,gly}$, the pathway through glycerol fermentation to 1,3-propanediol (Eq.S3, $k_{m,gly3}$) accounted for 65.8% of all pathways of glycerol degradation in Mechanism I, and 23.6% through glycerol fermentation to acetic acid and formic acid (Eq.S1, $k_{m,gly1}$). $k_{m,j}$ of glycerol fermentation processes in Mechanism II and III were also calculated (Fig. S2D and S2F). The glycerol degradation pathway of Mechanism II was same as that of Mechanism I. In Mechanism III, the pathway through glycerol fermentation to 1,3-propanediol (Eq.S3, $k_{m,gly3}$) was also the main degradation pathway of glycerol, accounting for 69.8%.

The maximum specific uptake rates of glycerol fermentation mentioned above and the maximum specific uptake rates of sulfate reduction using single organic compounds as electron donors (calculated in Section 3.2), combined with the k_s listed in the literature and those adjusted in this work in Section 3.1, were used for a validation

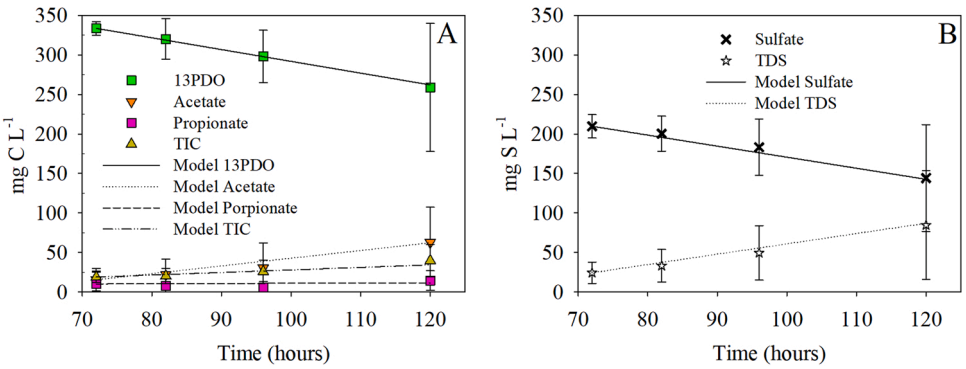

Fig. 4. Sulfate reduction with 1,3-propanediol as the electron donor in Mechanism I. Data points illustrate the experimental data. Smooth lines represent model predictions.

Table 4
Maximum specific uptake rates of each single organic compounds in Mechanism I, II and III. Confidence interval estimated through FIM is presented in parentheses.

	Mechanism I		Mechanism II and III		
Parameter	$k_{m,13PDO1}$	$k_{m,13PDO2}$	$k_{m,3HP1}$	$k_{m,3HP2}$	$k_{m,13PDO3}$
mg C mg VSS^{-1} h^{-1}	3.45 (± 0.01)	1.06 (± 0.01)	3.17 (± 0.18)	0.98 (± 0.09)	4.62 (± 0.42)

attempt performed by simulating Mechanism I and the batch test fed with glycerol and sulfate. Model predictions are shown in Fig. 5. As can be observed, the model prediction did not fit the experimental results. The production of 1,3-propanediol in the model was overestimated, while the production of ethanol and sulfate reduction were underestimated. Model predictions using Mechanism II and III (Figures not shown) resulted exactly the same as the mechanism I. Such mismatching was attributed to the contribution of other microbial communities on glycerol fermentation. Bryant et al. [46] demonstrated that sulfate reducer genus *Desulfovibrio* fermented lactate or ethanol to acetate in anaerobic ecosystems containing little or no sulfate. *Desulfobulbus* species are also capable of fermenting lactate and ethanol to acetate and propionate [47]. Plugge et al. [48] described that some sulfate reducers can shift their metabolism from sulfidogenic in presence of sulfate to acetogenic, hydrogenogenic metabolism in the absence of sulfate. It can be concluded that sulfate reducers can be metabolically active in anaerobic digestion without sulfate, which may explain the overestimation of 1,3-propanediol production. Due to the different affinity of SRB for different organic compounds, the incorrect estimation of glycerol fermentation products resulted in underestimation of sulfate reduction rate. Thus, the recalibration of maximum specific rates of glycerol fermentation in the presence of sulfate was necessary.

3.3.2. *Model calibration for glycerol fermentation coupled to sulfate reduction*

Maximum uptake rates of glycerol fermentation were recalibrated in the batch test fed with glycerol in the presence of sulfate, whereas the same $k_{m,j}$ for sulfate reduction processes calibrated in the sulfate reduction process with single organic compounds (Section 3.2) were used. The three mechanisms (I, II and III) were simulated and compared through Student's t-test and Fval to also decide which mechanistic approach provided a better prediction of the experimental data. In the simultaneous presence of glycerol and sulfate, the predicted profiles for each model variable are shown in Fig. 6. Fig. 6A shows that the model prediction of acetate concentration was significantly higher than the experimental data in Mechanism I, while the sulfate reduction rate and the production rate of TDS in the model were both higher than the experimental data (Fig. 6B). A significant difference ($P < 0.05$) between the experimental data and the model prediction was obtained and a Fval

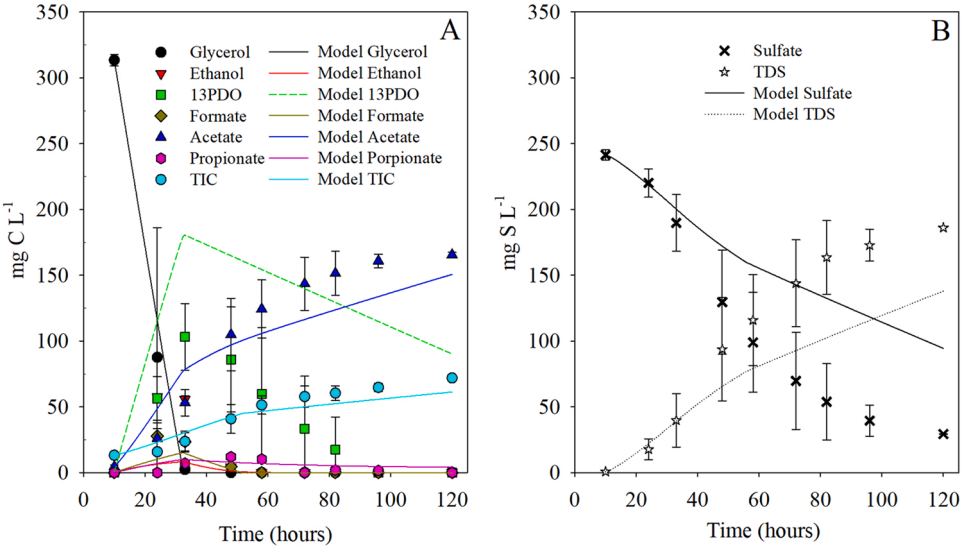

Fig. 5. Model validation of glycerol fermentation in presence of sulfate. A shows glycerol fermentation processes and B shows sulfate reduction process. Data points illustrate the experimental data. Smooth lines represent model predictions.

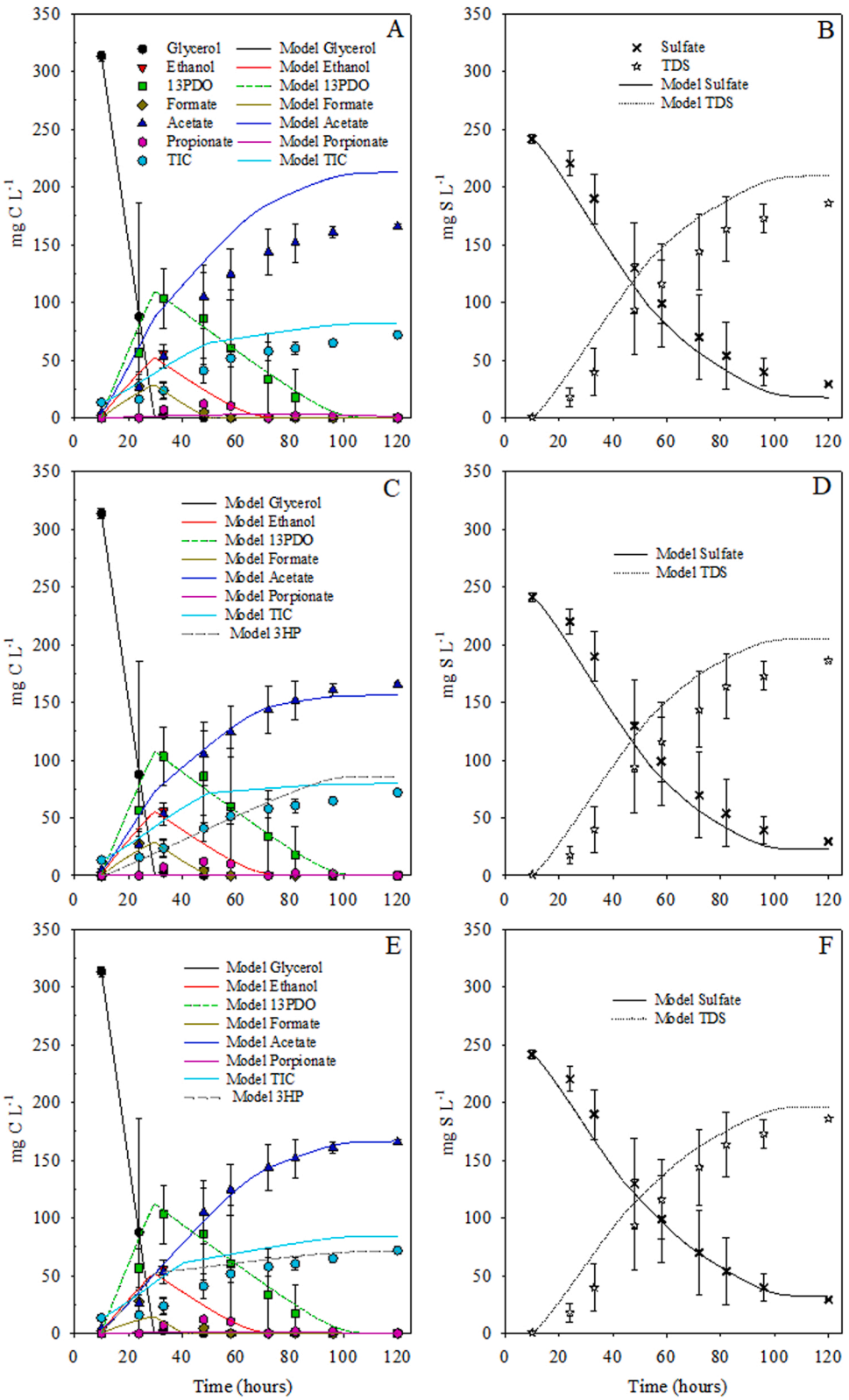

Fig. 6. Experimental and simulated profiles of sulfate reduction process using glycerol as carbon source in Mechanism I (A, B), Mechanism II (C, D), and Mechanism III (E, F). Data points illustrate the experimental data. Smooth curves represent model predictions.

of 250.4 was found in Mechanism I. Using Mechanism II (Fig. 6C and D), the Fval was 166.5, a 34% lower Fval than in Mechanism I. Student's t-test showed that there was no significant difference in carbon compounds concentration between the model and the experimental data (Fig. 6C). However, the model overestimated the sulfate reduction (Fig. 6D). Using Mechanism III (Fig. 6E and F), there was no significant difference between the model data and the experimental data in carbon (Fig. 6E) and sulfur compounds (Fig. 6F). The minimum error between model and experimental data was obtained in Mechanism III (Fval =152.0), which indicates that the mathematical model based on

Table 5
Monod maximum specific uptake rates of glycerol and 3-hydroxypropionate in Mechanism III. Confidence interval estimated through FIM is presented in parentheses.

Parameter	$k_{m,gly1}$	$k_{m,gly2}$	$k_{m,gly3}$	$k_{m,gly4}$	$k_{m,gly5}$	$k_{m,3HP1}$	$k_{m,3HP2}$
mg C mg VSS^{-1} h^{-1}	3.58 (± 0.07)	0.10 (± 0.07)	17.97 (± 0.01)	17.13 (± 0.04)	3.43 (± 0.06)	2.56 (± 0.02)	0.19 (± 0.03)

Mechanism III well-described the sulfate reduction process with glycerol as the electron donor, thus revealing that 3HP contributed to intermediate metabolite in the process of sulfate reduction during the glycerol fermentation and 1,3-propanediol degradation might be the main processes playing a role out of the 3 mechanisms compared herein. However, although the H_2S transferred from the liquid phase to the gas phase was considered in this model, the model predicted that the TDS in the liquid was still higher than the experimental data. This was attributed to the possible production of organic sulfur compounds during the activity test [49].

The mathematical model based on Mechanism III well-described the experimental data, and the parameters related to sulfate reduction processes were validated. In the presence of sulfate, the calibrated maximum uptake rates of glycerol fermentation ($k_{m,gly}$) and 3HP fermentation ($k_{m,3HP}$) of Mechanism III using glycerol as the electron donor are shown in Table 5. In Mechanism III, the pathway through glycerol fermentation to 13PDO (Eq.S3, $k_{m,gly3}$) and the pathway through glycerol fermentation to ethanol and formic acid (Eq.S4, $k_{m,gly4}$) were the main pathways of glycerol fermentation, accounting for 42.6% and 40.6%, respectively. This result agrees with previous studies [50, 51], in which ethanol and 1,3-propanediol were found as the main products of glycerol fermentation.

The present work verified the degradation pathway of glycerol by the model simulation. 3HP was produced during the process of 1,3-propanediol degradation in presence of sulfate [33], and it could be further mainly converted to acetate [32]. As shown in Table 5, the route through 3HP oxidized to acetate was the main route of 3HP degradation, accounting for up to 93.1%.

The confidence intervals of estimated parameters listed in Tables 3–5 were assessed according to the FIM method. In general, the relative errors associated to the estimated parameters were low (<9.1%) for k_m, except for $k_{m,gly1}$ and $k_{m,gly2}$. The maximum error calculated was $k_{m,gly1}$ (accounting for 70.0%, associated to glycerol fermented to acetic acid and formic acid). However, this fermentation pathway (associated to $k_{m,gly1}$) were not substantial in the glycerol fermentation process, accounting for 0.2%. Thus, the low confidence intervals indicate a high reliability of the estimated parameters in model predictions, which is also confirmed by the satisfactory description of the experimental behavior with the proposed kinetic model.

Previous kinetic models of anaerobic degradation of glycerol coupled to sulfate reduction, proposed by Dinkel et al. [26], were based on reactions in which glycerol was directly oxidized to acetate by fermentative bacteria and sulfate reducers. However, the present work showed that fermentation of glycerol contained a variety of intermediate products, including ethanol, 1,3-propanediol, propionate, acetate, carbonate, etc. that must be added to the modeling approach. The model proposed in this work considered a set of intermediate metabolites of glycerol fermentation that can reproduce experimental results in a highly consistent manner. Based on the results of a sensitivity analysis, the maximum specific uptake rates involved in the degradation of glycerol and sulfate reduction were calculated, in which the parameter $k_{m,j}$ of sulfate reduction were validated. The kinetic parameters calibrated herein could be useful for the long-term operation in anaerobic reactors. Although the mathematical model based on Mechanism III was in closer agreement with the experimental data, the role of 3HP must be experimentally verified in future works. Furthermore, the model should be further evolved in order to predict the competitive dynamics of the microbial community and their impact in the performance of biological anaerobic reactors.

4. Conclusion

A mathematical model describing sulfate reduction and anaerobic glycerol fermentation through multiple pathways and multiple intermediate products with sulfate reduction process was established and discussed. The model described glycerol degradation through the reductive and oxidative pathways. The kinetic parameters of the maximum specific uptake rates of substrate were calibrated and then, the sulfate reduction process was validated. The three proposed mechanisms were compared by fitting model to experimental data. It was found that the model established by Mechanism III was in higher agreement. In this mechanism, apart from considering the products ethanol, 1,3-propanediol, formate, acetate, propionate, and carbonate, 3HP was included as a metabolite in the fermentation of glycerol. Among them, the bioconversion of 1,3-propanediol and ethanol were the main pathway of glycerol fermentation, accounting for 42.6% and 40.6%, respectively. Moreover, it was determined that 3HP was an intermediate product of 1,3-propanediol degradation in the presence of sulfate.

CRediT authorship contribution statement

Xudong Zhou: Methodology, Software, Validation, Formal analysis, Investigation, Data curation, Writing – original draft, Writing – review & editing, Visualization. **Antoni D. Dorado:** Software, Validation, Formal analysis, Investigation, Resources, Writing – review & editing, Supervision. **Javier Lafuente:** Investigation, Data curation, Resources, Funding acquisition. **Xavier Gamisans:** Conceptualization, Validation, Formal analysis, Investigation, Writing – review & editing, Supervision, Project administration. **David Gabriel:** Conceptualization, Methodology, Validation, Investigation, Writing – review & editing, Supervision, Project administration, Funding acquisition.

Declaration of Competing Interest

The authors declare that they have no known competing financial interests or personal relationships that could have appeared to influence the work reported in this paper.

Acknowledgments

Authors are members of the GENOCOV research group from the Department of Chemical, Biological and Environmental Engineering at UAB (Universitat Autònoma de Barcelona), and the Department of Mining, Industrial and ICT Engineering, Universitat Politècnica de Catalunya. Authors acknowledge the Ministerio de Economía y Competitividad, Spanish Government, through the project RTI2018-099362-B-C21 and C22 MINECO/FEDER, EU, for the financial support provided to perform this research. The first author thanks the China Scholarship Council (CSC, 201706300052) for financial support.

Appendix A. Supporting information

Supplementary data associated with this article can be found in the online version at doi:10.1016/j.jece.2022.107937.

References

[1] Y. Gu, F. Jérôme, Glycerol as a sustainable solvent for green chemistry, Green Chem. 12 (2010) 1127–1138, https://doi.org/10.1039/c001628d.

[2] J.M. Naranjo, J.A. Posada, J.C. Higuita, C.A. Cardona, Valorization of glycerol through the production of biopolymers: The PHB case using *Bacillus megaterium*, Bioresour. Technol. 133 (2013) 38–44, https://doi.org/10.1016/j.biortech.2013.01.129.

[3] Y.Q. Sun, W.T. Qi, H. Teng, Z.L. Xiu, A.P. Zeng, Mathematical modeling of glycerol fermentation by *Klebsiella pneumoniae*: Concerning enzyme-catalytic reductive pathway and transport of glycerol and 1,3-propanediol across cell membrane, Biochem. Eng. J. 38 (2008) 22–32, https://doi.org/10.1016/j.bej.2007.06.002.

[4] G. Kaur, A.K. Srivastava, S. Chand, Bioconversion of glycerol to 1,3-propanediol: a mathematical model-based nutrient feeding approach for high production using *Clostridium diolis*, Bioresour. Technol. 142 (2013) 82–87, https://doi.org/10.1016/j.biortech.2013.05.040.

[5] C.V. Rodrigues, F.A. Rios Alcaraz, M.G. Nespeca, A.V. Rodrigues, F. Motteran, M. A. Tallarico Adorno, M.B.A. Varesche, S.I. Maintinguer, Biohydrogen production in an integrated biosystem using crude glycerol from waste cooking oils, Renew. Energy 162 (2020) 701–711, https://doi.org/10.1016/j.renene.2020.08.061.

[6] V. Beschkov, T. Sapundzhiev, I. Angelov, Modelling of biogas production from glycerol by anaerobic process in a baffled multi-stage digestor, Biotechnol. Biotechnol. Equip. 26 (2012) 3244–3248, https://doi.org/10.5504/bbeq.2012.0061.

[7] M. Mora, E. Fernández-Palacios, X. Guimerà, J. Lafuente, X. Gamisans, D. Gabriel, Feasibility of S-rich streams valorization through a two-step biosulfur production process, Chemosphere 253 (2020), 126734, https://doi.org/10.1016/j.chemosphere.2020.126734.

[8] P.N.L. Lens, A. Visser, A.J.H. Janssen, L.W. Hulshoff Pol, G. Lettinga, Biotechnological treatment of sulfate-rich wastewaters, Crit. Rev. Environ. Sci. Technol. 28 (1998) 41–88, https://doi.org/10.1080/10643389891254160.

[9] T. Alemu, E. Lemma, A. Mekonnen, S. Leta, Performance of pilot scale anaerobic-SBR system integrated with constructed wetlands for the treatment of tannery wastewater, Environ. Process. 3 (2016) 815–827, https://doi.org/10.1007/s40710-016-0171-1.

[10] D.B. Johnson, I. Sánchez-Andrea, Dissimilatory reduction of sulfate and zero-valent sulfur at low pH and its significance for bioremediation and metal recovery, Adv. Microb. Physiol. 75 (2019) 205–231, https://doi.org/10.1016/bs.ampbs.2019.07.002.

[11] T. Hao, P. Xiang, H.R. Mackey, K. Chi, H. Lu, H. Chui, M.C.M. van Loosdrecht, G.-H. Chen, A review of biological sulfate conversions in wastewater treatment, Water Res. 65 (2014) 1–21, https://doi.org/10.1016/j.watres.2014.06.043.

[12] D.J. Batstone, J. Keller, J.P. Steyer, A review of ADM1 extensions, applications, and analysis: 2002-2005, Water Sci. Technol. 54 (2006) 1–10, https://doi.org/10.2166/wst.2006.520.

[13] D.J. Batstone, D. Puyol, X. Flores-Alsina, J. Rodríguez, Mathematical modelling of anaerobic digestion processes: applications and future needs, Rev. Environ. Sci. Biotechnol. 14 (2015) 595–613, https://doi.org/10.1007/s11157-015-9376-4.

[14] P.Halkjaer Nielsen, Biofilm dynamics and kinetics during high-rate sulfate reduction under anaerobic conditions, Appl. Environ. Microbiol. 53 (1987) 27–32, https://doi.org/10.1128/aem.53.1.27-32.1987.

[15] A. Gupta, J.R.V. Flora, G.D. Sayles, M.T. Suidan, Methanogenesis and sulfate reduction in chemostats-II. Model development and verification, Water Res. 28 (1994) 795–803, https://doi.org/10.1016/0043-1354(94)90086-8.

[16] S. Kalyuzhnyi, V. Fedorovich, Integrated mathematical model of UASB reactor for competition between sulphate reduction and methanogenesis, Water Sci. Technol. 36 (1997) 201–208, https://doi.org/10.1016/S0273-1223(97)00524-6.

[17] S.V. Kalyuzhnyi, V.V. Fedorovich, Mathematical modelling of competition between sulphate reduction and methanogenesis in anaerobic reactors, Bioresour. Technol. 65 (1998) 227–242, https://doi.org/10.1016/S0960-8524(98)00019-4.

[18] D.J. Batstone, J. Keller, I. Angelidaki, S.V. Kalyuzhnyi, S.G. Pavlostathis, A. Rozzi, W.T. Sanders, H. Siegrist, V.A. Vavilin, The IWA Anaerobic Digestion Model No 1 (ADM1), Water Sci. Technol. 45 (2002) 65–73, https://doi.org/10.2166/wst.2002.0292.

[19] V. Fedorovich, P. Lens, S. Kalyuzhnyi, Extension of anaerobic digestion model No. 1 with processes of sulfate reduction, Appl. Biochem. Biotechnol. 109 (2003) 33–46, https://doi.org/10.1385/ABAB:109:1-3:33.

[20] E.L. Barrera, H. Spanjers, K. Solon, Y. Amerlinck, I. Nopens, J. Dewulf, Modeling the anaerobic digestion of cane-molasses vinasse: Extension of the Anaerobic Digestion Model No. 1 (ADM1) with sulfate reduction for a very high strength and sulfate rich wastewater, Water Res. 71 (2015) 42–54, https://doi.org/10.1016/j.watres.2014.12.026.

[21] H. Chen, J. Wu, B. Liu, Y. Li, H. Yasui, Competitive dynamics of anaerobes during long-term biological sulfate reduction process in a UASB reactor, Bioresour. Technol. 280 (2019) 173–182, https://doi.org/10.1016/j.biortech.2019.02.023.

[22] A.P. Zeng, K. Menzel, W.D. Deckwer, Kinetic, dynamic, and pathway studies of glycerol metabolism by *Klebsiella pneumoniae* in anaerobic continuous culture: II. Analysis of metabolic rates and pathways under oscillation and steady-state conditions, Biotechnol. Bioeng. 52 (1996) 561–571, https://doi.org/10.1002/(SICI)1097-0290(19961205)52:5<561::AID-BIT3>3.0.CO;2-H.

[23] J. Wang, J. Ye, H. Yin, E. Feng, L. Wang, Sensitivity analysis and identification of kinetic parameters in batch fermentation of glycerol, J. Comput. Appl. Math. 236 (2012) 2268–2276, https://doi.org/10.1016/j.cam.2011.11.015.

[24] J.F. Andrews, A mathematical model for the continuous culture of microorganisms utilizing inhibitory substrates, Biotechnol. Bioeng. 10 (1968) 707–723, https://doi.org/10.1002/bit.260100602.

[25] V.H. Edwards, The influence of high substrate concentrations on microbial kinetics, Biotechnol. Bioeng. 12 (1970) 679–712, https://doi.org/10.1002/bit.260120504.

[26] V.G. Dinkel, F.B. Frechen, A.V. Dinkel, Y.Y. Smirnov, S.V. Kalyuzhnyi, Kinetics of anaerobic biodegradation of glycerol by sulfate-reducing bacteria, Appl. Biochem. Microbiol. 46 (2010) 712–718, https://doi.org/10.1134/s0003683810070069.

[27] M.B. Viana, A.V. Freitas, R.C. Leitão, G.A.S. Pinto, S.T. Santaella, Anaerobic digestion of crude glycerol: a review, Environ. Technol. Rev. 1 (2012) 81–92, https://doi.org/10.1080/09593330.2012.692723.

[28] K.K. Cheng, J.A. Zhang, D.H. Liu, Y. Sun, H.J. Liu, M. De Yang, J.M. Xu, Pilot-scale production of 1,3-propanediol using *Klebsiella pneumoniae*, Process Biochem. 42 (2007) 740–744, https://doi.org/10.1016/j.procbio.2007.01.001.

[29] B. Yang, S. Liang, H. Liu, J. Liu, Z. Cui, J. Wen, Metabolic engineering of *Escherichia coli* for 1,3-propanediol biosynthesis from glycerol, Bioresour. Technol. 267 (2018) 599–607, https://doi.org/10.1016/j.biortech.2018.07.082.

[30] X. Zhou, E. Fernández-Palacios, A.D. Dorado, X. Gamisans, D. Gabriel, Assessing main process mechanism and rates of sulfate reduction by granular biomass fed with glycerol under sulfidogenic conditions, Chemosphere 286 (2022), 131649, https://doi.org/10.1016/J.CHEMOSPHERE.2021.131649.

[31] A.I. Qatibi, R. Bennisse, M. Jana, J.-L. Garcia, Anaerobic degradation of glycerol by *Desulfovibrio fructosovorans* and *D. carbinolicus* and evidence for glycerol-dependent utilization of 1,2-Propanediol, Curr. Microbiol. 36 (1998) 283–290, https://doi.org/10.1007/s002849900311.

[32] A.I. Qatibi, J.L. Cayol, J.L. Garcia, Glycerol and propanediols degradation by *Desulfovibrio alcoholovorans* in pure culture in the presence of sulfate, or in syntrophic association with *Methanospirillum hungatei*, FEMS Microbiol. Lett. 85 (1991) 233–240, https://doi.org/10.1111/j.1574-6968.1991.tb04729.x.

[33] A.I. Qatibi, V. Nivière, J.L. Garcia, *Desulfovibrio alcoholovorans* sp. nov., a sulfate-reducing bacterium able to grow on glycerol, 1,2- and 1,3-propanediol, Arch. Microbiol. 155 (1991) 143–148, https://doi.org/10.1007/BF00248608.

[34] E. Fernández-Palacios, X. Zhou, M. Mora, D. Gabriel, Microbial diversity dynamics in a methanogenic-sulfidogenic UASB reactor, Int. J. Environ. Res. Public Health 18 (2021) 1305, https://doi.org/10.3390/ijerph18031305.

[35] O. Gutierrez, D. Park, K.R. Sharma, Z. Yuan, Effects of long-term pH elevation on the sulfate-reducing and methanogenic activities of anaerobic sewer biofilms, Water Res. 43 (2009) 2549–2557, https://doi.org/10.1016/J.WATRES.2009.03.008.

[36] A. Visser, L.W. Hulshoff Pol, G. Lettinga, Competition of methanogenic and sulfidogenic bacteria, Water Sci. Technol. 33 (1996) 99–110, https://doi.org/10.1016/0273-1223(96)00324-1.

[37] A. Zeng, A. Ross, H. Biebl, C. Tag, B. Günzel, W. Deckwer, B. Gunzel, Multiple product inhibition and growth modeling of *Clostridium butyricum* and *Klebsiella pneumoniae* in glycerol fermentation, Biotechnol. Bioeng. 44 (1994) 902–911, https://doi.org/10.1002/bit.260440806.

[38] B.M. Gonzalez-Silva, R. Briones-Gallardo, E. Razo-Flores, L.B. Celis, Inhibition of sulfate reduction by iron, cadmium and sulfide in granular sludge, J. Hazard. Mater. 172 (2009) 400–407, https://doi.org/10.1016/j.jhazmat.2009.07.022.

[39] P. Dornseiffer, B. Meyer, E. Heinzle, Modeling of anaerobic formate kinetics in mixed biofilm culture using dynamic membrane mass spectrometric measurement, Biotechnol. Bioeng. 45 (1995) 219–228, https://doi.org/10.1002/bit.260450306.

[40] D. Dochain, P.A. Vanrolleghem, Dynamical modelling and estimation in wastewater treatment processes, 2001.

[41] A. Guisasola, J.A. Baeza, J. Carrera, G. Sin, P.A. Vanrolleghem, J. Lafuente, The Influence of experimental data quality and quantity on parameter estimation accuracy, Educ. Chem. Eng. 1 (2006) 139–145, https://doi.org/10.1205/ece06016.

[42] A.D. Dorado, G. Baquerizo, J.P. Maestre, X. Gamisans, D. Gabriel, J. Lafuente, Modeling of a bacterial and fungal biofilter applied to toluene abatement: Kinetic parameters estimation and model validation, Chem. Eng. J. 140 (2008) 52–61, https://doi.org/10.1016/j.cej.2007.09.004.

[43] M. Mora, L.R. López, J. Lafuente, J. Pérez, R. Kleerebezem, M.C.M. van Loosdrecht, X. Gamisans, D. Gabriel, Respirometric characterization of aerobic sulfide, thiosulfate and elemental sulfur oxidation by S-oxidizing biomass, Water Res. 89 (2016) 282–292, https://doi.org/10.1016/j.watres.2015.11.061.

[44] G.A. Vignolle, C. Simon, G.A. Vignolle, C. Derntl, T. Tomin, K. Novak, R.L. Mach, R. Birner-grünberger, S. Pflügl, A quantitative metabolic analysis reveals *Acetobacterium woodii* as a flexible and robust host for formate-based bioproduction, Metab. Eng. 68 (2021) 68–85, https://doi.org/10.1016/j.ymben.2021.09.004.

[45] M.F.M. Bijmans, E. de Vries, C.H. Yang, C.J.N. Buisman, P.N.L. Lens, M. Dopson, Sulfate reduction at pH 4.0 for treatment of process and wastewaters, Biotechnol. Prog. 26 (2010) 1029–1037, https://doi.org/10.1002/btpr.400.

[46] M.P. Bryant, L.L. Campbell, C.A. Reddy, M.R. Crabill, Growth of *Desulfovibrio* in lactate or ethanol media low in sulfate in association with H_2 utilizing methanogenic bacteria, Appl. Environ. Microbiol. 33 (1977) 1162–1169, https://doi.org/10.1128/aem.33.5.1162-1169.1977.

[47] G. Muyzer, A.J.M. Stams, The ecology and biotechnology of sulphate-reducing bacteria, Nat. Rev. Microbiol. 6 (2008) 441–454, https://doi.org/10.1038/nrmicro1892.

[48] C.M. Plugge, W. Zhang, J.C.M. Scholten, A.J.M. Stams, Metabolic flexibility of sulfate-reducing bacteria, Front. Microbiol. 2 (2011) 81, https://doi.org/10.3389/fmicb.2011.00081.

[49] M. Mora, J. Lafuente, D. Gabriel, Influence of crude glycerol load and pH shocks on the granulation and microbial diversity of a sulfidogenic Upflow Anaerobic Sludge

Blanket reactor, Process Saf. Environ. Prot. 133 (2020) 159–168, https://doi.org/10.1016/j.psep.2019.11.005.

[50] S. Sittijunda, A. Reungsang, Fermentation of hydrogen, 1,3-propanediol and ethanol from glycerol as affected by organic loading rate using up-flow anaerobic sludge blanket (UASB) reactor, Int. J. Hydrogen Energy 42 (2017) 27558–27569, https://doi.org/10.1016/j.ijhydene.2017.05.149.

[51] D.M. Rossi, J.B. da Costa, E.A. de Souza, M. do, C.R. Peralba, M.A.Z. Ayub, Bioconversion of residual glycerol from biodiesel synthesis into 1,3-propanediol and ethanol by isolated bacteria from environmental consortia, Renew. Energy 39 (2012) 223–227, https://doi.org/10.1016/j.renene.2011.08.005.